

# Simulations of optical inner-channel thermal deformation for high-power system with unstable resonator

Ruhai Guo (郭汝海)<sup>1\*</sup>, Wei Tang (汤伟)<sup>1,2</sup>, Bin Wang (王兵)<sup>1</sup>,  
Kui Shi (时魁)<sup>1</sup>, and Ning Chen (陈宁)<sup>1</sup>

<sup>1</sup>State Key Laboratory of Laser Interaction with Matter, Changchun Institute of Optics and Physics, Chinese Academy of Sciences, Changchun 130033, China

<sup>2</sup>University of Chinese Academy of Sciences, Beijing 100049, China

\*Corresponding author: hitgrh@163.com

Received January 27, 2013; accepted March 2, 2013; posted online August 15, 2013

In this letter, the influence on the beam quality due to cumulative effect of the inner channel thermal deformation in the high energy laser system with unstable resonator is researched. Firstly, three typical laser powers of 50, 100, and 150 kW are selected to analyze thermal deformation of mirror by the finite element analyze of thermodynamics instantaneous method. Then the wave front aberration can be calculated by ray-tracing theory. Finally, Strehl ratio and Zernike aberration coefficients of the vacuum far-filed beam can be calculated and comparably analyzed by Fresnel diffraction integration. The theory and simulation results show that due to the effect of inner channel thermal deformation, eccentric phenomenon and astigmatism of far-filed beam emerge, and peak power and the focused ability decrease. With the increasing of reflective times, Strehl ratio decrease, and tilt, astigmatism and coma of  $x$  direction gradually increase, which become the main aberration. The results can provide the reference to the thermal aberration analysis for high energy laser system and can be applied to the field of laser nuclear fusion and laser weapon, etc.

OCIS codes: 140.3410, 140.6810.

doi: 10.3788/COL201311.S21402.

It has gain a great attention from all over the world for wide applications of high-energy laser system<sup>[1–3]</sup>. But there always exists heat absorption of laser when the high-energy laser beam passes through the optical elements of beam control system (inner-channel), which will make the wave front of laser beam distortion. Furthermore, this effect will cumulate as the increasing optical elements. This will ultimately influence the far-field optical beam quality.

At present, many research groups have paid great attention for the heat distortion of mirror irradiated by high-energy laser<sup>[4–6]</sup>. However, there are rarely reports about the heat distortion of mirror influencing the far-field optical beam quality. The researches mostly focus

on the heat distortion of single mirror or output window of laser cavity, not including multiple mirrors which built up the real inner-channel of laser system. At the same time, the optical intensity distribution of high-energy laser beam is usually generated by the unstable resonator which is hollow in center and asymmetry<sup>[7]</sup>. Therefore, it is necessary to investigate the heat distortion of inner-channel for high-energy laser system, especially the influence of far-field optical beam quality.

Based on the heat distortion of single mirror, the model of inner-channel is established to analyze the effect of heat distortion influencing the far-field beam quality in this letter. In the unstable resonator, the ring top-flat Gaussian beam is formulated as

$$E' = E_0 \left\{ \exp \left[ -\frac{(N+1)(x^2+y^2)}{w^2} \right] \times \sum_{n=0}^N \frac{1}{n!} \left[ \frac{(N+1)(x^2+y^2)}{w^2} \right]^n - \exp \left[ -\frac{(N+1)(x^2+y^2)}{w_0^2} \right] \times \sum_{n=0}^N \frac{1}{n!} \left[ \frac{(N+1)(x^2+y^2)}{w_0^2} \right]^n \right\}, \quad (1)$$

where  $N$  is the order of top-flat Gaussian beam,  $w$  is the radii of outer ring,  $w_0$  is the radii of inner ring. The asymmetry of beam and increase with the output power of laser. Because the intensity distribution of optical beam along the flow field direction of the gain medium is inhomogeneous, the asymmetry of beam will increase with the increasing output power of laser. Therefore the expression of optical intensity distribution of unstable resonator can be simply expressed as<sup>[8]</sup>

$$E = E' \left( 1 - \frac{x}{s} \right), \quad (2)$$

where  $s$  is the intercept of the  $x$  direction. It can

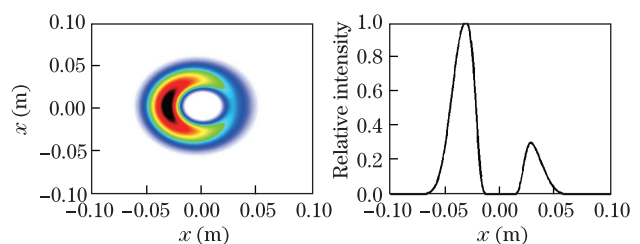


Fig. 1. (Color online) Optical intensity distribution of unstable resonator.

describe the degree of asymmetry, which take  $s=0.1$  in our simulation work. The beam intensity formation is shown in Fig. 1.

When the high-energy beam irradiates the optical elements, mostly refer to mirrors. There must be small fraction of laser energy to be absorbed by the mirror, which makes the mirror temperature increasing. The temperature field of mirror can be expressed as<sup>[9]</sup>

$$\begin{aligned} \frac{\partial}{\partial x} \left[ k(T) \frac{\partial T}{\partial x} \right] + \frac{\partial}{\partial y} \left[ k(T) \frac{\partial T}{\partial y} \right] \\ + \frac{\partial}{\partial z} \left[ k(T) \frac{\partial T}{\partial z} \right] = \rho c \frac{\partial T}{\partial t}, \end{aligned} \quad (3)$$

where  $T$  is the temperature of  $t$  time at the point  $(r, \phi, z)$  of mirror,  $k$  is the coefficient of heat exchange for the material of mirror,  $\rho$  is the density of mirror, and  $c$  is the specific heat. The temperature field of mirror is influenced by three factors: heat injection, heat exchange, and heat convection with the ambient atmosphere. Therefore, the boundary condition is

$$\begin{cases} k \frac{\partial T}{\partial n} |_{\Sigma} = -[(1 - \varepsilon) I(r, \phi) / S - h_c (T_s - T_c)] \\ k \frac{\partial T}{\partial n} |_{\Sigma_1} = h_c (T_s - T_c) \\ T_c = 20 \text{ } ^\circ\text{C} \\ T_s |_{t=0} = 20 \text{ } ^\circ\text{C} \end{cases}, \quad (4)$$

where  $T_c$  is the ambient temperature,  $T_s$  is the surface temperature of mirror,  $h_c$  is the coefficient of convection heat exchange,  $\varepsilon$  is the reflectivity of mirror,  $I(r, \phi)$  is the optical intensity of laser,  $S$  is the area of irradiation,  $\Sigma$  is the load region of laser beam distribution, and  $\Sigma_1$  is the load region of heat convection. Substituting Eq. (4) into Eq. (3), the temperature distribution of mirror can be obtained under the high-energy laser irradiation.

In this letter, a 220-mm-diameter silicon mirror is chosen with 15-mm thickness and 99% reflectivity. The other material parameters are listed in the Table 1. The thermal distortion caused by the temperature gradient can be described by the thermal-elastic equations<sup>[10]</sup>:

$$\begin{cases} \nabla^2 u_r - \frac{u_r}{r^2} + \frac{1}{1-2\nu} \frac{\partial e}{\partial r} - \frac{2(1+\nu)}{1-2\nu} \alpha_t \frac{\partial T}{\partial r} = 0 \\ \nabla^2 u_z + \frac{1}{1-2\nu} \frac{\partial e}{\partial z} - \frac{2(1+\nu)}{1-2\nu} \alpha_t \frac{\partial T}{\partial z} = 0 \end{cases}, \quad (5)$$

where  $u_r$  and  $u_z$  are the radial and axial thermal distortion of mirror,  $e$  is the thermal strain of mirror,  $\alpha_t$  is the coefficient of heat expanding for the substrate material, and  $\nu$  is the Poisson's ratio. The boundary condition of mirror is supposed fixed in its circumference, as

$$u_r |_{r=r_0} = u_z |_{r=r_0} = 0. \quad (6)$$

There are many numerical methods to solve Eqs. (1)–(5), such as the method of finite difference, the method of finite element and the method of fast Fourier transform etc. Here we adopt the software of finite element (Ansys) to analyze the temperature distribution of single mirror and its thermal distortion. Then using Zernike polynomial to fit the distortion displacement of mirror and can be corresponding to the aberrance items. The

single mirror irradiated by the above laser beam is shown as Fig. 2 where  $r$  is the radius of the mirror,  $h$  is the thickness of the mirror, and  $\theta$  is the incidence angle.

When the laser beam reflects from the mirror with the thermal distortion, there will add an additional

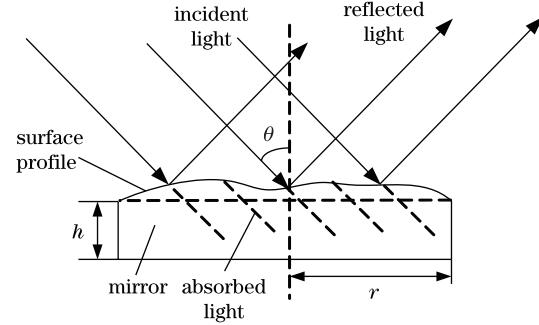


Fig. 2. Thermal deformation of single mirror.

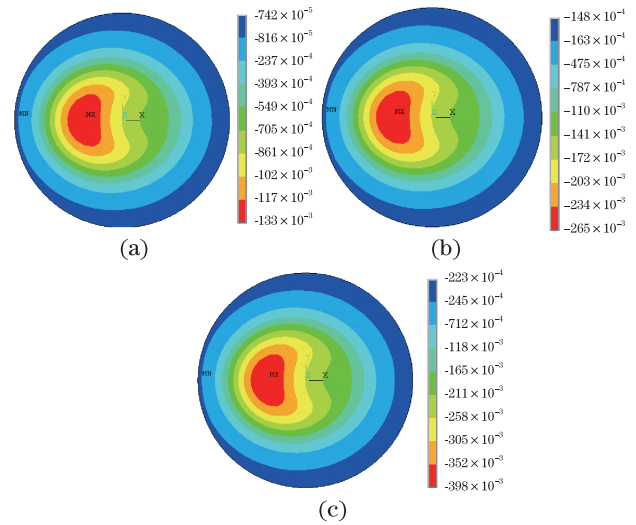


Fig. 3. (Color online) Thermal distortion of the mirror with the increasing of laser powers of (a) 50; (b) 100; (c) 150 kW.

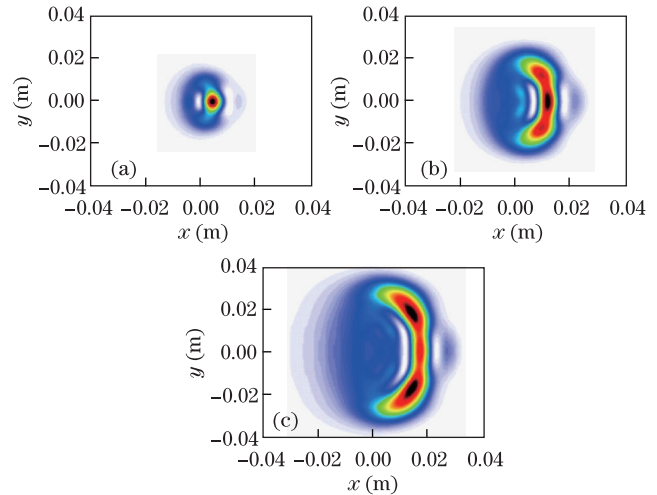


Fig. 4. (Color online) Far-field optical intensity distribution of non-uniform laser after 15 times 45° reflection. (a) 50; (b) 100; (c) 150 kW.

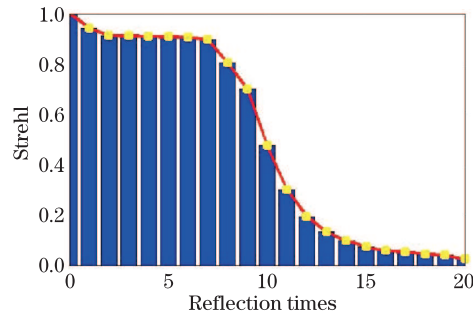


Fig. 5. (Color online) Strehl ratio with the different reflection times.

phase  $\phi(x, y)$ . Therefore, the light amplitude after the reflection is expressed as

$$U_1(x, y) = U_0(x, y) \exp[i\phi(x, y)]. \quad (7)$$

In the simulation,  $\lambda=10.6 \mu\text{m}$ ,  $N=4$ ,  $w=0.05 \text{ m}$ ,  $w_0=0.02 \text{ m}$ , under the boundary condition, using the parameters of Table 1, the irradiation time is 5 s, and the laser powers are 50, 100, and 150 kW, respectively. The thermal distortion of the mirror is shown as Fig. 3.

With increasing the laser power, the thermal distortion also increases and the maximum distortion is about  $3.98 \mu\text{m}$ , which equals  $\lambda/3$  ( $\lambda=10.6 \mu\text{m}$ ). This thermal distortion cannot be neglected because the typical root mean square (RMS) of a mirror is less than  $\lambda/10$ . If the inner-channel consists of 15 same mirrors and 1 m

between each mirror, the far-field optical intensity distribution with the same laser powers are shown in Fig. 4.

The whole thermal distortion has no matter with the layout of each mirror, and it can be regarded as the wavefront aberration of single mirror multiplying the reflection times<sup>[11]</sup>. Due to the thermal distortion accumulation, the laser spot size and the eccentricity increase with the laser power enhance from 50 to 150 kW. In the real engineering, through Zernike polynomial fitting the wavefront of optical beam, we can obtain different aberration items.  $Z_1$  is constant item,  $Z_2$  and  $Z_3$  are tilting items,  $Z_4$  is defocus item,  $Z_5$  and  $Z_6$  are astigmatism items,  $Z_7$  and  $Z_8$  are coma items, and  $Z_9$  is third order spherical aberration. The relationship between the aberration items and the reflective times is listed in Table 2.

From Table 2, with increasing the reflective times, the astigmatism, the tilting, the coma increase at the same time in the  $x$  direction. But the astigmatism in the  $y$  direction gradually decreases. In high-power laser system, the Strehl ratio of the optical beam quality is mostly concerned for the far-field energy focus. The simulation results are shown in Fig. 5.

Under the same laser power, with the increasing reflection times, the Strehl ratio begins to drop. Especially, when the reflection times are more than 7, the ratio drop dramatically, which means that the cumulative wavefront aberration is larger than  $2\pi$ . Therefore, in the processing of design, the mirrors of inner-channel and the reflective times are also

Table 1. Parameters of Material Silicon

Density ( $\text{kg}/\text{m}^3$ )	Specific Heat ( $\text{J}/\text{kg} \cdot ^\circ\text{C}$ )	Heat Exchange Coefficient ( $\text{W}/\text{m} \cdot \text{K}$ )	Line Coefficient ( $/^\circ\text{C}$ )	Poisson's Ratio	Elastic Module ( $\text{N}/\text{m}^2$ )
2329	695	153	$4.68 \times 10^{-6}$	0.26	$1.9 \times 10^{11}$

Table 2. Front Nine Zernike Coefficients With Different Reflective times

Reflective Times	$Z_1$	$Z_2$	$Z_3$	$Z_4$	$Z_5$	$Z_6$	$Z_7$	$Z_8$	$Z_9$
1	0.127	-0.463	-0.724	0.119	0.572	3.436	-0.134	-0.241	-0.120
8	0.127	-0.463	-0.724	0.119	0.577	3.434	-0.134	-0.240	-0.120
10	0.109	-1.216	-0.663	0.107	0.194	3.592	-0.405	-0.216	-0.099
13	0.069	-2.216	-0.480	0.077	-1.931	3.302	-0.770	-0.149	-0.055
15	0.037	-2.729	-0.316	0.052	-3.745	2.788	-0.961	-0.092	-0.022
20	-0.032	-3.201	0.093	-0.007	-5.664	0.869	-1.146	0.048	0.048

the important factor to influence the far-field optical beam quality. If the inner-channel including more than 7 mirrors in this example, the control techniques of thermal deformation is essential.

In conclusion, the inner-channel thermal deformation is theoretically analyzed. The simulation results show that the laser power and the reflection times are the key factors to influence the far-field optical beam quality when the material and the boundary are determined. The astigmatism and the tilting phenomenon become the main effect to decrease the far-field optical beam quality with increasing the laser power and reflective times. There exists a special inflexion reflective time, which is more than the time that needs the control techniques to

restrain this thermal distortion. The results provide the reference for the optical beam control of entire path of the high-power laser system.

This research was supported by the Natural Science Foundation of Jilin Province, China (No. 201115123) and the Jilin Province Nature Science Fund and the State Key Laboratory Independence Foundation Project (Nos. 201115123 and SKLLIM1004-01).

## References

1. G. P. Perran, M. A. Marciniak, and M. Goda, Proc. SPIE **5414**, 1 (2004).
2. K. N. LaFortune, R. L. Hurd, S. N. Fochs, M. D. Rot-

- ter, P. H. Pax, R. L. Combs, S. S. Olivier, J. M. Brase, and R. M. Yamamoto, Proc. SPIE **6454**, 64540O (2007).
3. H. J. Kong, J. W. Yoon, and J. S. Shin, Proc. SPIE **6454**, 64540C (2007).
  4. P. Lu and Y. Wang, Chin. J. Lasers (in Chinese) **29**, 201 (2002).
  5. Y. Peng, Z. Cheng, Y. Zhang, C. Zhou, W. Yu, Y. Lu, and F. Li, Chin. J. Lasers (in Chinese) **29**, 21 (2002).
  6. Z. Feng, L. Bai, Z. Zhang, and G. Lin, Opt. Precision Eng. **18**, 1781 (2010).
  7. C. Zhou and Z. Cheng, High Power Laser Part. Beams (in Chinese) **15**, 969 (2003).
  8. H. T. Ma, Q. Zhou, X. J. Xu, S. J. Du, and Z. J. Liu, Opt. Express **19**, 1037 (2011).
  9. Y. Du, J. An, and X. Shu, High Power Laser Part. Beams (in Chinese) **20**, 1333 (2008).
  10. Y. Su and M. Wan, *High Energy Laser System* (in Chinese) (National Defense Industry Press, Beijing, 2004) pp. 1-9.
  11. W. Liu, P. Rao, and W. Hua, High Power Laser Part. Beams (in Chinese) **20**, 1615 (2008).